Translational Oncology 47 (2024) 102040

Contents lists available at ScienceDirect

Translational Oncology

journal homepage: www.elsevier.com/locate/tranon

Original Research

CuET overcomes regorafenib resistance by inhibiting epithelial-mesenchymal transition through suppression of the ERK pathway in hepatocellular carcinoma

Ding Ma [1,a,c,d], Shuwen Liu [1,a,b,c], Kua Liu [1,a,b,c], Qinyu He [a,b,c], Lili Hu [c], Weiwei Shi [a,b,c], Yin Cao [a,c], Guang Zhang [a,c], Qilei Xin [a,b], Zhongxia Wang [a,c,*], Junhua Wu [a,b,*], Chunping Jiang [a,b,c,*]

[a] Jinan Microecological Biomedicine Shandong Laboratory, Jinan, Shandong 250117, China
[b] State Key Laboratory of Pharmaceutical Biotechnology, National Institute of Healthcare Data Science at Nanjing University, Jiangsu Key Laboratory of Molecular Medicine, Medical School, Nanjing University, 22 Hankou Road, Nanjing, Jiangsu, 210093 China
[c] Department of Hepatobiliary Surgery, the Affiliated Drum Tower Hospital of Nanjing University Medical School, Nanjing 210008, China
[d] Department of Gastroenterology, Third Xiangya Hospital, Central South University, Changsha, Hunan, China

ARTICLE INFO

Keywords:
HCC
Regorafenib
Regorafenib-resistant MHCC-97H
CuET
Reversal of regorafenib resistance

ABSTRACT

Background and Purpose: Regorafenib was approved by the US Food and Drug Administration (FDA) for hepatocellular carcinoma (HCC) patients showing progress on sorafenib treatment. However, there is an inevitably high rate of drug resistance associated with regorafenib, which reduces its effectiveness in clinical treatment. Thus, there is an urgent need to find a potential way to solve the problem of regorafenib resistance. The metabolite of disulfiram complexed with copper, the Diethyldithiocarbamate-copper complex (CuET), has been found to be an effective anticancer drug candidate. In the present study, we aimed to evaluate the effect of CuET on regorafenib resistance in HCC and uncover the associated mechanism.

Experimental Approach: Regorafenib-resistant HCC strains were constructed by applying an increasing concentration gradient. This study employed a comprehensive range of methodologies, including the cell counting kit-8 (CCK-8) assay, colony formation assay, cell cycle analysis, wound healing assay, Transwell assay, tumor xenograft model, and immunohistochemical analysis. These methods were utilized to investigate the antitumor activity of CuET, assess the combined effect of regorafenib and CuET, and elucidate the molecular mechanism underlying CuET-mediated regorafenib resistance.

Key Results: The inhibitory effect of regorafenib on cell survival, proliferation and migration was decreased in regorafenib-resistant MHCC-97H (MHCC-97H/REGO) cells compared with parental cells. CuET demonstrated significant inhibitory effects on cell survival, proliferation, and migration of various HCC cell lines. CuET restored the sensitivity of MHCC-97H/REGO HCC cells to regorafenib in vitro and in vivo. Mechanistically, CuET reverses regorafenib resistance in HCC by suppressing epithelial-mesenchymal transition (EMT) through inhibition of the ERK signaling pathway.

Conclusion and Implications: Taken together, the results of this study demonstrated that CuET inhibited the activation of the ERK signaling pathway, leading to the suppression of the epithelial-mesenchymal transition (EMT) and subsequently reversing regorafenib resistance in HCC both in vivo and in vitro. This study provides a new idea and potential strategy to improve the treatment of regorafenib-resistant HCC.

Introduction

As one of the most common malignant tumors among humans worldwide, hepatocellular carcinoma (HCC) has the characteristics of high mortality and high metastasis potential. The 5-year relative survival rate of HCC patients is only 33 % and has not increased

* Corresponding authors.
E-mail addresses: freud_t@126.com (Z. Wang), wujunhua@nju.edu.cn (J. Wu), chunpingjiang@nju.edu.cn (C. Jiang).
[1] These authors contributed equally to this work.

https://doi.org/10.1016/j.tranon.2024.102040
Received 15 August 2023; Received in revised form 11 January 2024; Accepted 20 June 2024

significantly over the past years [1]. Surgical treatment, including microwave ablation, liver resection and liver transplantation, is the most important approach for the treatment of HCC [2], but many patients have already lost the opportunity for surgical treatment by the time they are diagnosed with HCC and can only opt for other treatment options [3, 4]. Molecularly targeted therapy seems to be the major method to prolong life in these patients [5-7].

Regorafenib is an FDA-approved oral multikinase inhibitor that can target multiple genes, including KIT, RAF1, BRAF, and VEGFR [8]. Figure S1 shows the structure of regorafenib. Regorafenib is considered to improve clinical outcomes in patients with unresectable HCC who have developed resistance to the first-line targeted drug sorafenib [9, 10]. The median survival of patients treated with regorafenib was 10.6 months (95 % CI 9.1–12.1) versus 7.8 months (6.3–8.8) for patients given a placebo. However, the clinical benefit was limited among the patients receiving regorafenib treatment, and their median time to progress (TTP) was only 4.5 months [5], which means that drug resistance is still an obstacle for regorafenib treatment. Therefore, it is of great practical significance to elucidate the underlying mechanism of regorafenib resistance in HCC and find appropriate treatments to overcome regorafenib resistance in HCC.

Epithelial-mesenchymal transition (EMT) is a cellular process in which adherent epithelial cells are converted to individual migratory cells [11], and it plays a central role in various pathological processes, including wound healing, carcinoma progression, tumor metastasis and drug resistance [12]. There is considerable evidence that due to the activation of EMT, systemic therapy often fails to eradicate carcinoma cells, resulting in clinical relapse [13-15]. Blocking EMT critically contributes to overcoming resistance to various therapeutic agents in multiple cancer types [14]. Wang et al. also demonstrated that reducing EMT reversed regorafenib resistance in HCC [16]. All of these results indicate that targeting EMT may be a promising strategy for the clinical treatment of regorafenib-resistant HCC.

Extracellular signal-related kinase (ERK) is the most important member of the MAPK signaling pathway. It regulates diverse cellular processes, such as proliferation, migration, metastasis, and resistance to chemotherapy. ERK cooperatively activates the EMT programme in various cancer types [14,17] and is considered a central driver of tumor progression [18]. Ma et al. showed that the induction of EMT via MEK1/ERK/ELK1 signaling in HCC can promote oxaliplatin resistance [19]. In addition, the RAS/RAF/MEK/ERK pathway is also known to play an essential role in the therapeutic drug resistance of HCC and prostate cancer [20,21]. Therefore, ERK-mediated EMT may be an important factor affecting the resistance of regorafenib in HCC. It also provides inspiration for selecting ERK pathway-targeting drugs that can improve or reverse regorafenib resistance in HCC.

Disulfiram (DSF), an FDA-approved drug for the treatment of “alcohol dependence”, has been proven to be a chemotherapeutic drug for cancer treatment [22,23]. The Diethyldithiocarbamate-copper complex (CuET) is the ultimate anticancer metabolite of DSF both in vivo and in vitro [24] and has shown greater antitumor efficacy than the original DSF. Figure S1 shows the structure of CuET. It is very attractive to reuse an old drug for new purposes, such as cancer treatment, and DSF is a good example of this approach due to its low cost, few side effects and high selectivity against different cancers [25]. Skrott et al. reported that patients who used DSF continuously had a lower risk of death [24]. DSF has been reported to potently inhibit the cell migration and invasion of HCC and breast cancer cells via the ERK pathway [26-28]. DSF has also already been used to overcome the resistance of bortezomib and cytarabine in acute myeloid leukemia cells [29]. In addition, CuET has shown a prominent capability to promote apoptosis and inhibit metastasis by inhibiting EMT in breast cancer [30]. Because of the inhibitory effect of CuET on the EMT and ERK pathways, CuET might overcome regorafenib resistance as a safe medication by affecting the EMT and ERK pathways.

In the present study, we aimed to investigate regorafenib resistance in HCC. To achieve this goal, we established regorafenib-resistant cell lines (MHCC-97H/REGO) using a concentration gradient increment method. To understand the cellular changes after acquiring resistance, we conducted various experiments to observe the malignant phenotypic changes in the resistant cells. To explore the role of ERK in this process, we also performed experiments by applying an ERK inhibitor to the resistant cells. Furthermore, we conducted experiments both in vitro and in vivo to assess the ability of CuET to reverse regorafenib resistance. Therefore, our findings will reveal the possible mechanism by which HCC cells acquire regorafenib resistance and the feasibility of reversing regorafenib resistance by inhibiting the EMT program and the ERK pathway.

Materials and methods

Generation of regorafenib-resistant HCC cells

Regorafenib-resistant HCC strains were constructed by using an increasing concentration gradient, in which the initial concentration of regorafenib was 5 μM and the concentration was increased by 0.5 μM per week. The concentration was increased in this manner as long as the cells continued to grow steadily, and the passage ability was normal after each increase in concentration. Culture growth was continued until the concentration at which the cell viability decreased. Subculture was carried out as described above, and the medium was replaced once a day during subculture. After 6 months of continuous stimulation, regorafenib-resistant HCC cell lines (IC_{50}: 13.78 ± 1.02 μM) were obtained and preserved in DMEM with 4 μM regorafenib.

Cell culture and processing

The HCC cell lines SMCC-7721, MHCC-97H and MHCC-LM3 were obtained from the Type Culture Collection of the Shanghai Cell Bank of the Chinese Academy of Sciences. The cells were cultured in DMEM (100 U/ml penicillin–streptomycin and 10 % fetal bovine serum) at 37 °C with 5 % CO_2. The MHCC-97H/REGO cell line was cultured in DMEM containing 4 μM regorafenib.

Cytotoxicity assay

The cytotoxicity of regorafenib was measured by the CCK-8 assay. HCC cells were plated in 96-well culture plates at a concentration of 10^5 cells/well and treated with regorafenib or CuET. After 72 h, 10 μL of CCK-8 solution was added, the cells were incubated for 1 h, and the absorbance was read at 450 nm on a multiwell plate reader.

Cell cycle

The cells were gently washed twice with sterile PBS, followed by digestion using an adequate volume of trypsin solution. A total of 5×10^5 cells were harvested through cell counting. The resulting cell suspension was placed in a sterile centrifuge tube, centrifuged at 1000 rpm for 5 min, and subjected to three subsequent washes and centrifugations to obtain a cell pellet. Subsequently, appropriate reagents were introduced according to the instructions provided with the cell cycle assay kit. Flow cytometry was employed to analyze the cells. Each experiment was independently repeated at least three times.

Colony formation assay

Cancer cells were seeded in 6-well culture plates at a concentration of 2×10^3 cells/well and then incubated in 5 % CO_2 at 37 °C. Cells were treated with DMEM containing regorafenib or CuET for 1 day and then with DMEM alone for 6 days. After 6 days, the colonies were fixed with 4 % paraformaldehyde for 1 h and stained with 0.5 % crystal violet for 20 min successively. Finally, the number of colonies was counted, and

photos were taken. Each experiment was independently repeated at least three times.

Wound healing assay

A total of 2×10^5 cells were seeded per well in a 24-well plate for 24 h. After a scratch wound was generated by scratching the cells vertically with a 200-μL pipette tip, the DMEM was replaced with serum-free medium containing the indicator. Images of the wound fields were acquired at 0, 24 or 48 h after incubation. The healing rates were calculated by the formula Area 0 h-Area x h/Area 0 h through ImageJ. The experiment was performed in triplicate.

Transwell assay

A total of 8×10^4 cells were suspended in serum-free specified medium and seeded into the upper chamber of a Boyden chamber (well) with a pore size of 8 μm (BD Biosciences) in 24-well Transwell plates. The upper chamber was filled with 300 μL of cell suspension, while the lower chamber was filled with 1 mL of specified medium containing 10 % FBS. After invading the lower chamber, the cells were fixed with 4 % paraformaldehyde and stained with crystal violet at room temperature for 1 h after they had incubated at 37 °C for 24 h. Cells were randomly photographed and counted in five microscopic fields.

Western blot analysis

Cells were collected and lysed in NP40 buffer (150 mM NaCl, 0.5 % EDTA, 50 mM Tris, 0.5 % NP40) and centrifuged at 12,000×*g* and 4 °C for 15 min. Ten or twenty micrograms of harvested total protein was loaded and separated on an 8, 10 or 12 % SDS-polyacrylamide gradient gel. The proteins were then transferred to polyvinylidene difluoride membranes and blocked with 5 % nonfat milk at room temperature for 2 h. The membranes were incubated with primary antibodies overnight at 4 °C, followed by incubation with HRP-conjugated secondary antibodies at room temperature for 2 h. After washing three times in TBST, the protein bands were observed using an enhanced chemiluminescence (ECL) system (Bio-Rad). Primary antibodies against the following proteins were used: vimentin (CST, 1:1000), snail (CST, 1:1000), phospho-p44/42 MAPK (CST, 1:1000), cyclin B1 (Biogot Technology, 1:1000), ERK1/2 (Biogot Technology, 1:1000), N-cadherin (CST, 1:1000), E-cadherin (CST, 1:1000), and GAPDH (Biogot Technology, 1:1000).

Immunohistochemical

Samples were fixed using a 4 % formaldehyde solution and subsequently embedded in paraffin. The paraffin-embedded tissue was then sectioned into 4 μm slices. For sample incubation at 4 °C, primary antibodies against E-cadherin, N-cadherin, vimentin, snail, cyclin B1, and phospho-p44/42 MAPK were applied, for an incubation time of 12 h. Subsequently, the slices underwent incubation at room temperature using an HRP-conjugated secondary antibody for 1 hour. Detection of the samples was achieved through 3,3′-diaminobenzidine and hematoxylin staining methods. Each experiment was repeated.

In vivo tumor experiments

MHCC-97H/REGO cells were harvested and washed twice with PBS. Approximately 1×10^7 cells were injected into the right forelimb armpit of each mouse after resuspension in 100 μL of PBS. Tumor size was measured and recorded every other day after the first treatment. Tumor volume was calculated as follows: tumor volume $= (L \times W^2)/2$ (L, maximum diameter; W, minimum diameter). Animal experiments were approved by the Animal Ethical and Welfare Committee of NJU (IACUC——D2202067). All protocols complied with the National Institutes of Health Guide for the Care and Use of Laboratory Animals (NIH Publications No. 8023, revised 1978).

Results

Characterization of regorafenib-resistant HCC cells

Long-term exposure of MHCC-97H cells to gradually increasing concentrations of regorafenib led to the emergence of regorafenib-resistant cells (MHCC-97/REGO). Compared to the MHCC-97H parent cells, the MHCC-97H/REGO cells become more mesenchymal exhibited an enlargement in cell size, a more rounded morphology (Fig. 1A). The MHCC-97H and MHCC-97H/REGO cell lines were treated with different concentrations of regorafenib for 72 h, and the CCK-8 assay was used to determine the sensitivity of the cell lines to regorafenib. The half-maximal inhibitory concentration (IC_{50}) of regorafenib in MHCC-97H/REGO cells was higher than that in the corresponding parent MHCC-97H cells. The IC_{50} was 13.78 ± 1.02 μM for MHCC-97H/REGO versus 7.16 ± 0.46 μM for MHCC-97H (Fig. 1B). Clonal formation experiments showed that the proliferation ability of the MHCC-97H/REGO cell line was stronger than that of the parental MHCC-97H cell line because MHCC-97H/REGO cells had more clones than MHCC-97H cells did ($p < 0.001$) (Fig. 1C and 1D). The cell cycle distribution showed a decrease in the percentage of MHCC-97H/REGO cells in the G2/M phase ($p < 0.05$) (Fig. 1E and 1F). Transwell (migration, $p < 0.001$; invasion, $p < 0.001$) and wound healing (24 h, $p < 0.05$; 48 h, $p < 0.05$) experiments showed that the migration ability of the MHCC-97H/REGO cell line was significantly greater than that of the MHCC-97H/REGO cell line (Fig. 1G-1 J). These results demonstrated the establishment of stable regorafenib-resistant HCC cell line and suggested that regorafenib-resistant HCC cells displayed increased mesenchymal, invasive, metastatic and proliferative phenotypes.

To identify the mechanisms and key effectors of regorafenib resistance, we performed protein microarray and differential gene expression analysis (Fig. 2A). The sequencing results confirmed previous findings showing that the cell cycle and EMT-related genes were more abundant in MHCC-97H/REGO cells than in MHCC-97H cells (Fig. 2B and 2C). At the same time, we found that the MAPK pathway was activated in MHCC-97H/REGO cells (Fig. 2C). The level of p-ERK in MHCC-97H/REGO cells was also significantly higher than that in control MHCC-97H cells (Fig. 2D and 2E). Therefore, we preliminarily hypothesized that p-ERK might cause such phenotypic changes, which will be verified in subsequent experiments. Similarly, the EMT markers N-cadherin, snail and vimentin were significantly upregulated, E-cadherin was significantly downregulated, and the cell cycle marker cyclin B1 was also significantly upregulated in the MHCC-97H/REGO cell line (Fig. 2D and 2E). This may also be the cause of regorafenib resistance in HCC.

The p-ERK inhibitor SCH772984 inhibits the proliferation and migration of MHCC-97H/REGO cells

To further understand the relationship between p-ERK and proliferation and migration in the MHCC-97H/REGO cell line, we inhibited the expression of p-ERK by using SCH772984 (a highly selective and ATP-competitive ERK inhibitor) [31]. SCH772984 significantly suppressed the expression of p-ERK, but not that of t-ERK (Fig. 3A). The IC_{50} value of regorafenib in MHCC-97H/REGO cells was decreased by SCH772984. The IC_{50} of MHCC-97H/REGO was 13.78 ± 1.02 μM, while the IC50 of MHCC-97H/REGO treated with SCH772984 was 7.501 ± 0.77 μM (Fig. 3B). Downregulation of p-ERK by SCH772984 significantly inhibited growth and promoted G2/M-phase arrest in MHCC-97H/REGO cells (colony formation, $p < 0.01$; cell cycle, $p < 0.01$) (Fig. 3C and 3D). Moreover, the invasion and migration capacities of MHCC-97H/REGO cells were inhibited after SCH772984 treatment (Transwell migration assay, $p < 0.001$; Transwell invasion assay, $p < 0.001$; wound-healing migration assay, $p < 0.001$) (Fig. 3E and 3F). The treatment of MHCC-97H/REGO cells with SCH772984 was

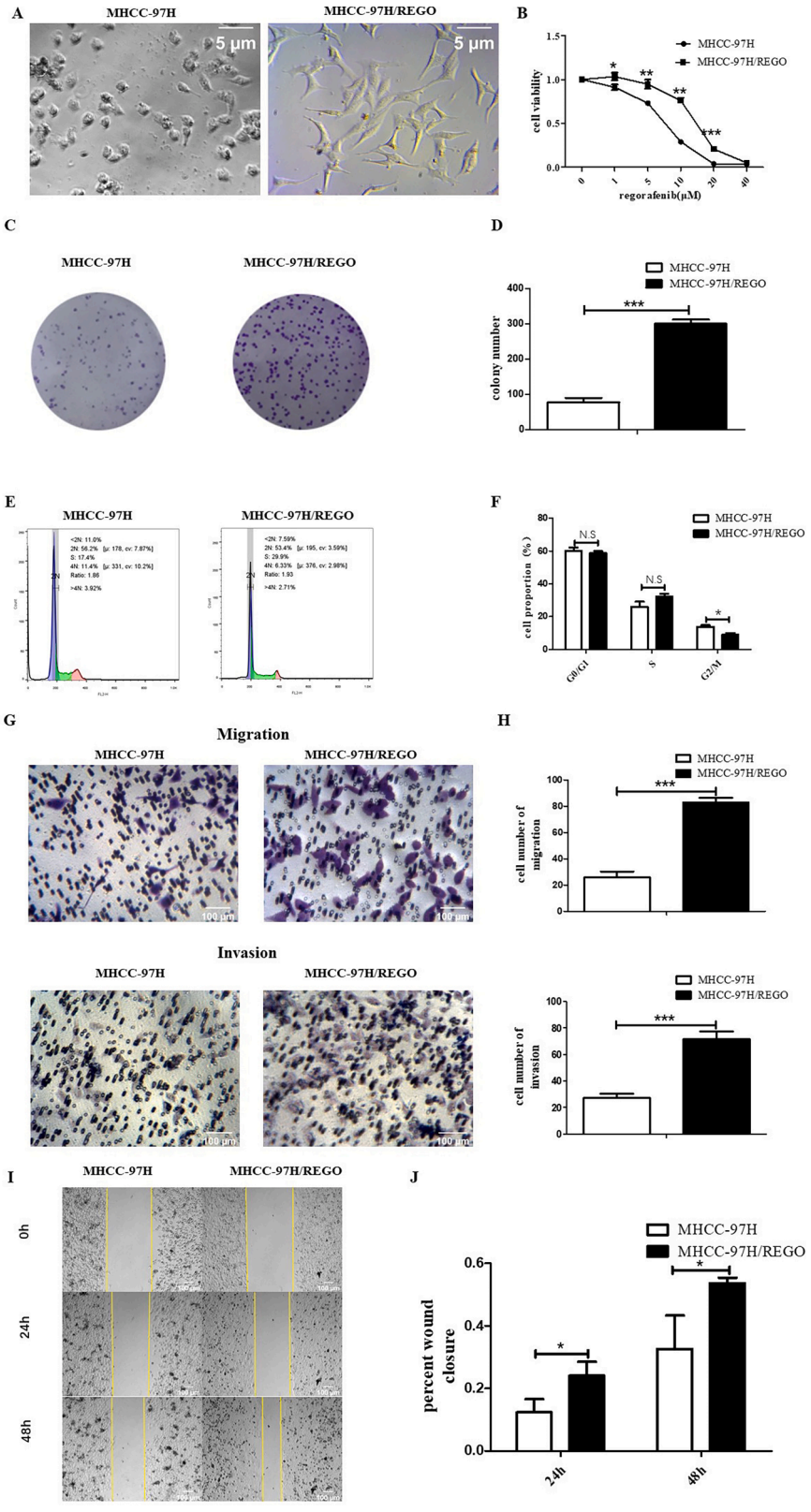

(caption on next page)

Fig. 1. In vitro characterization of regorafenib-resistant cells.
A. MHCC-97H/REGO cells showed a fibroblast-like and mesenchymal morphology. MHCC-97H and MHCC-97H/REGO cells were photographed with a microscope at 100× magnification. B. MHCC-97H and MHCC-97H/REGO cells were treated with different concentrations of regorafenib for 72 h. Cell viability was determined by the CCK-8 assay. The IC_{50} values for MHCC-97H and MHCC-97H/REGO were 7.16 ± 0.46 μM and 13.78 ± 1.02 μM, respectively. C-D. Colony formation experiments with MHCC-97H and MHCC-97H/REGO cells after cell culture for 7 days. Cells were plated at a density of 10^3 cells per well. E-F. Flow cytometry analysis was conducted to examine the cell cycle distribution of MHCC-97H/REGO and MHCC-97H cells. G-H. The migration and invasion abilities of MHCC-97H and MHCC-97H/REGO cells were determined by Transwell experiments. In each group, 8×10^4 cells were plated, and the number of cells passing through the Transwell chamber was recorded 24 h later. I-J. Migration ability of MHCC-97H and MHCC-97H/REGO cells was determined by wound-healing migration assays. Photos were taken after 0 h, 24 h and 48 h of culture, after which the healing rate was calculated. $^*p < 0.05$, $^{**}p < 0.01$, $^{***}p < 0.001$ (one-way ANOVA).

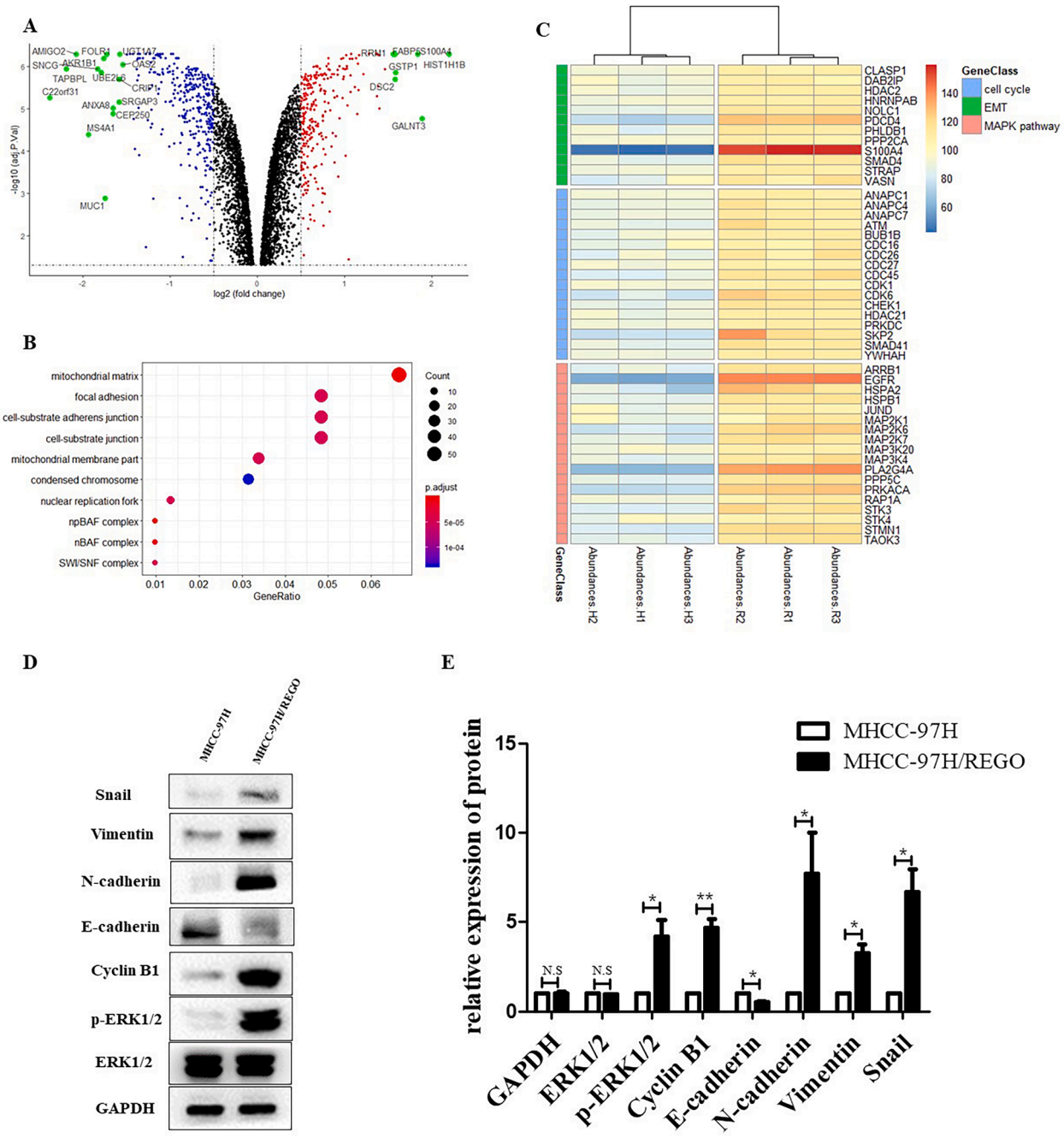

Fig. 2. Changes in protein abundance in regorafenib-resistant cells compared to parental cells.
A. Volcano plot for differential gene expression. B. GO analysis of the DEGs in the MHCC-97H/REGO cohort. C. Heatmap of protein microarray data for cell cycle, EMT and MAPK pathway genes in the MHCC-97H and MHCC-97H/REGO cell lines. d-E. Qualitative and quantitative analysis of the protein expression levels of E-cadherin, N-cadherin, vimentin, snail, cyclin B1, p-ERK and t-ERK in MHCC-97H and MHCC-97H/REGO cells.

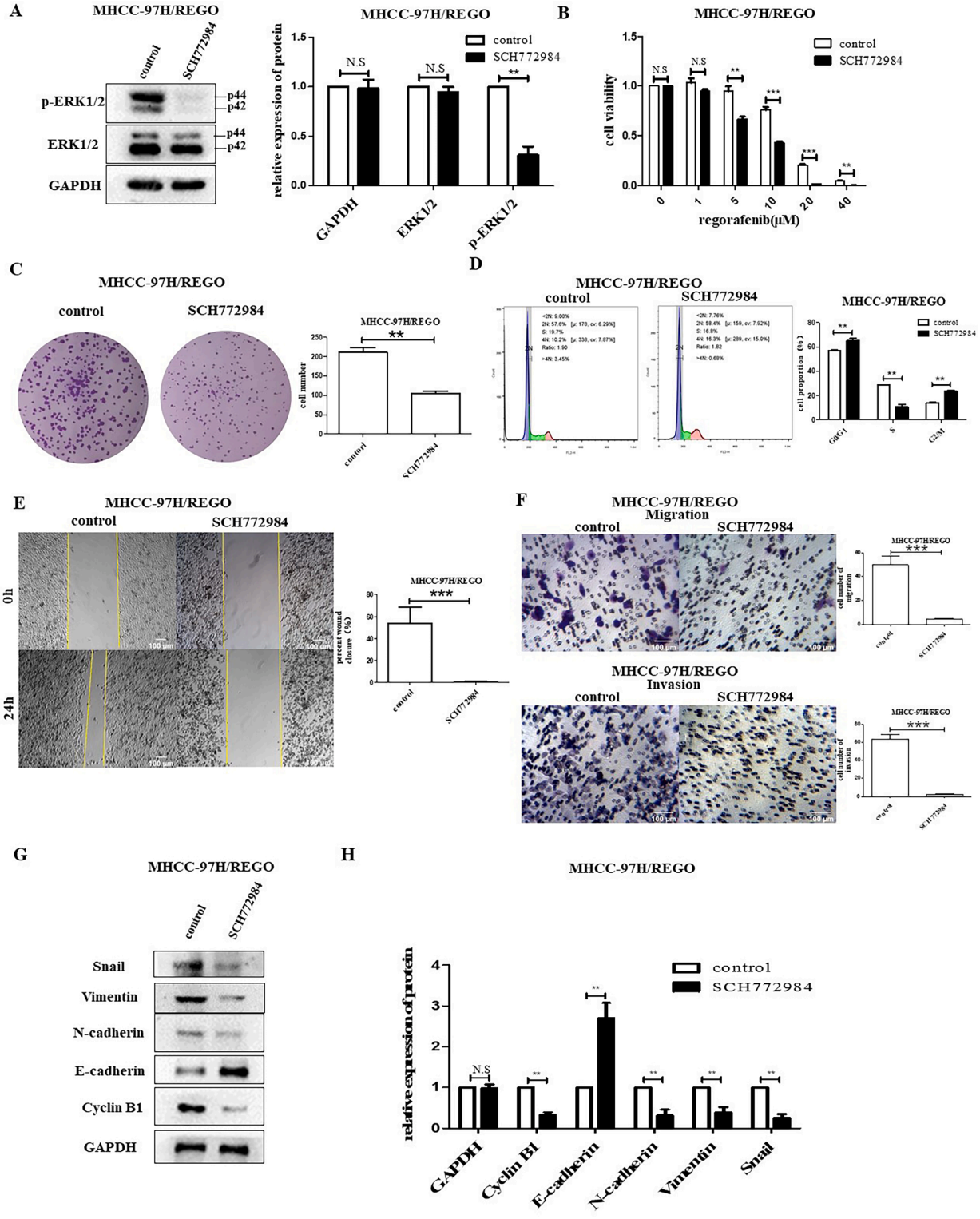

Fig. 3. Effect of p-ERK on regorafenib resistance in the MHCC-97H/REGO cell line.
A. The expression of t-ERK and p-ERK in MHCC-97H/REGO cells treated with SCH772984. B. Cell viability was determined by the CCK-8 assay. The IC_{50} values for MHCC-97H/REGO- and SCH772984-treated MHCC-97H/REGO cells were 13.78 ± 1.02 μM and 7.501 ± 0.77 μM, respectively. C. Colony formation ability of MHCC-97H/REGO cells treated with or without the p-ERK inhibitor SCH772984 (5 μM). Cells were plated at a density of 10^3 per well and then treated with vehicle or SCH772984 for 24 h. D. Cell cycle distributions of SCH772984 treated MHCC-97H/REGO cells. E. Wound healing experiments in MHCC-97H/REGO cells treated with (right) or without (left) SCH772984 (5 μM). F. The migration and invasion ability of MHCC-97H/REGO cells were determined by Transwell experiments. A total of 8 × 10^4 cells were implanted into the Transwell chamber and treated with vehicle or SCH772984 (5 μM) for 24 h. G-H. Qualitative and quantitative analyses of the protein levels of E-cadherin, N-cadherin, vimentin, snail, cyclin B1, p-ERK and t-ERK in MHCC-97H/REGO cells were performed via western blotting. Cells were treated with (right) or without (left) SCH772984 (5 μM) for 24 h. *$p < 0.05$, **$p < 0.01$, ***$p < 0.001$ (one-way ANOVA).

accompanied by a decrease in the levels of the EMT markers vimentin and N-cadherin, as well as the cell cycle marker cyclin B1 (Fig. 3G and 3H). The present study confirmed that upregulation of p-ERK may be responsible for regorafenib resistance.

CuET potently inhibits p-ERK in a regorafenib-resistant HCC cell line and HCC cell lines

In the present study, we found that p-ERK expression was closely related to regorafenib resistance (Fig. 2). Therefore, we tested the effect of CuET on p-ERK in regorafenib-resistant HCC cells and normal HCC cells. In this study, we found that CuET significantly inhibited p-ERK expression in the MHCC-97H/REGO, MHCC-97H, SMCC-7721 and MHCC-LM3 cell lines (Fig. 4A). The results verified the pronounced effect of CuET on reversing regorafenib resistance. Based on these results, we decided to further investigate the potential of CuET to reverse regorafenib resistance in subsequent experiments.

CuET potently inhibits the proliferation of a regorafenib-resistant HCC cell line and HCC cell lines via G2/M cell cycle arrest

To investigate whether CuET has the ability to overcome regorafenib resistance, CCK-8 assays were performed to investigate the cytotoxic effects of CuET on the regorafenib-resistant HCC cell line and normal HCC cell lines: MHCC-97H/REGO, MHCC-97H, MHCC-LM3 and SMCC-7721 (Fig. 4B). Cell viability was significantly inhibited by treatment with 0.1 μM to 0.5 μM CuET for 24 h in MHCC-97H/REGO, MHCC-97H, MHCC-LM3 and SMCC-7721 cells. A colony formation assay was further performed to verify the antiproliferative effect of CuET in a regorafenib-resistant HCC cell line and HCC cell lines (Fig. 4C). Cell proliferation was significantly inhibited after treatment with 0.05 or 0.1 μM CuET for 24 h. Cell cycle and Western blot analysis revealed that treatment with CuET for 24 h arrested the cell cycle in the G2/M-phase and suppressed the expression of cyclin B1 in these cells (Fig. 4D). All of these results indicate the inhibitory effect of CuET on HCC cell proliferation via G2/M cell cycle arrest.

CuET potently inhibits the migration and invasion of a regorafenib-resistant HCC cell line and HCC cell lines

To investigate the anti-metastatic potential of CuET, we used MHCC-97H/REGO, MHCC-97H, SMCC-7721 and MHCC-LM3 cells to explore the effect of CuET on HCC cell migration and invasion. In the scratch-wound healing recovery assay (24 h, 48 h) and Transwell assay (24 h), the wound healing (24 h, $p < 0.05$; 48 h, $p < 0.001$), migration (24 h) and invasion (24 h) abilities of the HCC cells were significantly inhibited by CuET (0.1 μM) (Fig. 4E and 4F). The EMT markers vimentin, snail and N-cadherin were also downregulated by CuET (0.1 μM), and E-cadherin was upregulated by CuET (0.1 μM) (Fig. 4G). These results indicated that CuET significantly inhibits the EMT process and migration in HCC cells.

CuET improves the effect of regorafenib on the drug-resistant MHCC-97H-derived cell line MHCC-97H/REGO in vitro

To further confirm the potential of CuET to overcome regorafenib resistance, we cultured MHCC-97H/REGO cells with CuET (0.1 μM, 0.15 μM or 0.2 μM) for the indicated times and then treated the MHCC-97H/REGO cells with regorafenib at different concentrations for the indicated times. With increasing CuET concentration, the cell viability of MHCC-97H/REGO decreased in a gradient, and MHCC-97H/REGO cells treated with a concentration of 0.2 μM CuET had significantly lower cell viability than did the control group or other experimental groups treated with lower concentrations of CuET (Fig. 5A). The IC_{50} values of regorafenib in MHCC-97H/REGO cells cocultured with CuET (0 μM, 0.1 μM, 0.15 μM, 0.2 μM) were 13.77 μM, 7.38 μM, 0.42 μM and 0.15 μM, respectively, indicating that MHCC-97H/REGO cells pretreated with CuET at a higher concentration were more sensitive to regorafenib (Fig. 5B). Then, we established four groups (control, regorafenib treatment, CuET treatment, and combined regorafenib and CuET treatment) to determine whether combination treatment with both drugs dramatically suppressed the proliferation and migration of tumors. The colony formation experiments showed a decreased number of colonies in the combination treatment group, which revealed that combination therapy had the greatest effect on decreasing cell proliferation among the four groups (Fig. 5C and 5D). Cell cycle analysis verified that the combination treatment had a synergistic effect on G2/M cell cycle arrest (Fig. 5E and 5F). Wound healing experiments also showed that the migration ability of MHCC-97H/REGO in the combination group was the worst (Fig. 5G and 5H). Transwell assays verified that the combination treatment had the lowest cell migration and invasion frequency (Fig. 5I and 5J).

Moreover, treatment with CuET reversed EMT in MHCC-97H/REGO cells by downregulating the EMT markers vimentin, snail and N-cadherin, upregulating E-cadherin, and downregulating the cell cycle marker cyclin B1 (Fig. 5K and 5L). These changes also indicate that CuET can restore the sensitivity of MHCC-97H/REGO cells to regorafenib.

CuET improved the effect of regorafenib on the drug-resistant MHCC-97H-derived cell line MHCC-97H/REGO in vivo

In addition, similar results were observed in vivo experiments; nude mice bearing MHCC-97H/REGO tumors were randomly grouped and treated with control, CuET (50 mg/kg DSF and 0.2 mg/kg CuGlu), regorafenib (20 mg/kg), or combination treatment. We found that the tumor volume in the combination therapy group was significantly lower than that in the other groups (Fig. 6A). There was no significant difference in body weight between the groups (Fig. 6B). After the tumor volume in the control group reached 1500 mm^3, the mice were euthanized, and the tumors were collected and photographed (Fig. 6C). The combination treatment group also had the lowest final tumor weight (Fig. 6D). Immunohistochemical results showed that the expression of the EMT markers vimentin, snail and N-cadherin, and the cell cycle marker cyclin B1 was low in the combination treatment group. Similarly, E-cadherin was high in the combination treatment group in vivo. This showed the high synergistic antitumor efficacy of the drug combination of regorafenib and CuET in vivo.

Discussion

Regorafenib is the first drug approved for the treatment of patients with HCC who progress during or after sorafenib therapy [32]. Unfortunately, as a second-line drug for HCC treatment, regorafenib also faces the risk of drug resistance [10]. Thus, some researchers are trying to reveal the resistance mechanism of regorafenib in HCC treatment [33], and others are trying to find drugs that can overcome regorafenib resistance in HCC treatment. This is the first study to prove that CuET can reverse regorafenib resistance in the treatment of HCC by inhibiting EMT via downregulation of the ERK pathway.

In the present study, the long-term culture of cells with regorafenib contributed to the acquisition of regorafenib resistance in the MHCC-97H cell line. We observed that the regorafenib-resistant cell line MHCC-97H/REGO grew and spread faster than MHCC-97H. In the study of Xiangping Song et al., faster growth was also observed in a regorafenib-resistant cell line of colon cancer [34]. Mustafa Karabicici et al. also generated drug-resistant cells from Huh7 cells, and they found that acquired resistance was associated with enhanced anti-apoptotic ability of the cells. They discovered that this resistance was mediated by TGF-β. As ERK also regulates TGF-β, this finding is not in conflict with our study but rather complements the understanding of the mechanism underlying regorafenib resistance in HCC [35].

In the present study, EMT occurred in MHCC-97H/REGO cells. During EMT, not only migration but also drug resistance is increased.

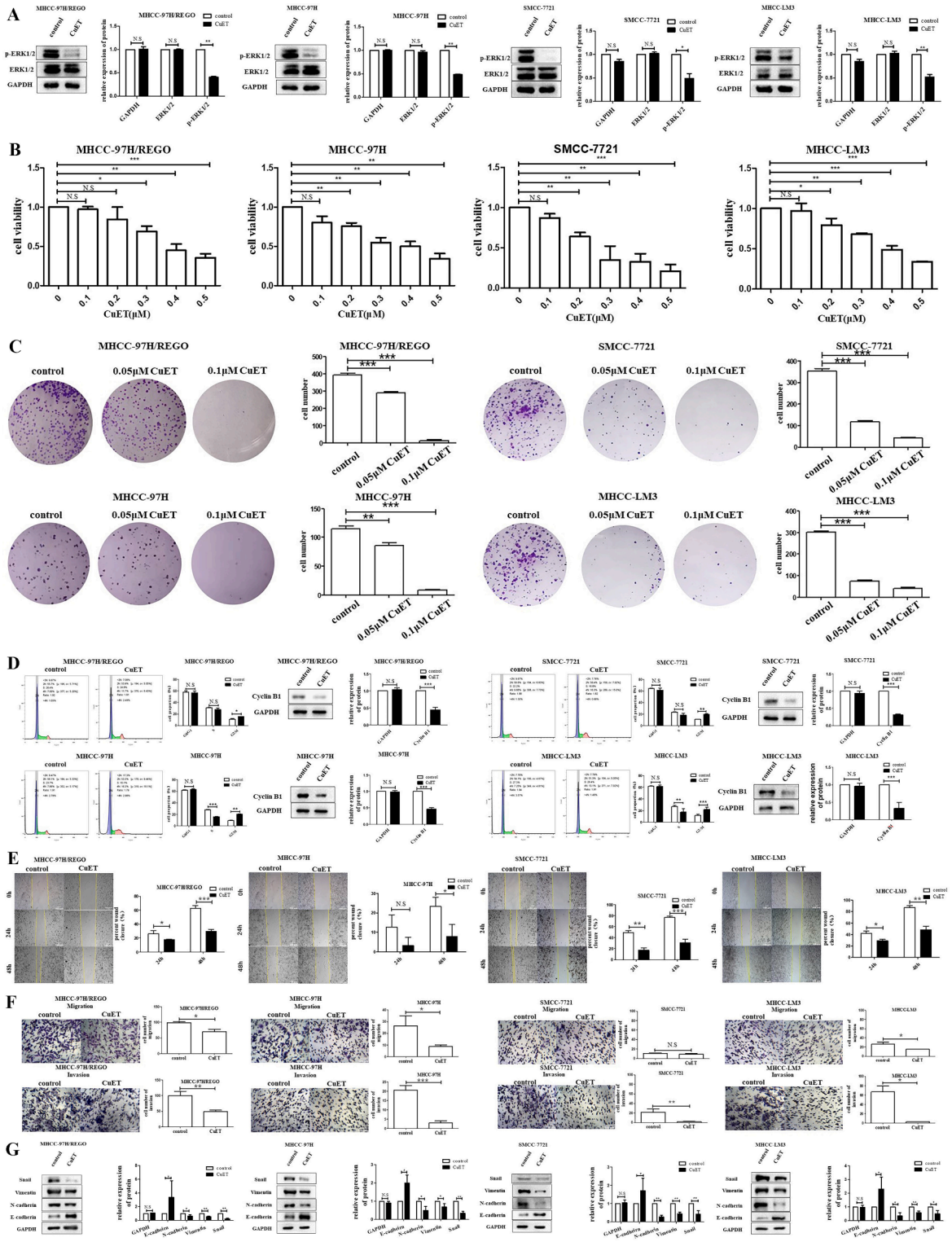

Fig. 4. Effect of CuET on the ERK pathway, and the proliferation, migration and invasion properties of different HCC cells.
A. Qualitative and quantitative analyses of p-ERK levels in MHCC-97H/REGO, MHCC-97H, SMCC-7721, and MHCC-LM3 cells by western blot. Total protein was extracted after the cells were treated with or without CuET (0.1 μM) for 24 h. B. The viability of MHCC-97H/REGO, MHCC-97H, SMCC-7721 and MHCC-LM3 cells exposed to the indicated concentrations of CuET for 24 h was determined by the CCK-8 assay. Cells were plated in 96-well plates at a density of 10^3 cells per well. C. Colony formation assay of MHCC-97H/REGO, MHCC-97H, SMCC-7721 and MHCC-LM3 cells. Cells were plated at a density of 10^3 cells per well and treated with vehicle or CuET at the indicated concentration for 24 h. The treatment-containing medium was then replaced with medium alone for 6 days. D. Cell cycle distributions of different CuET-treated HCC cell lines. Qualitative and quantitative analyses of the expression of cyclin B1 in different HCC cell lines treated with or without CuET (0.1 μM) for 24 h by western blotting. E. Wound healing experiments were performed on different HCC cell lines for 0 h, 24 h and 48 h. Cells were treated with or without CuET (0.1 μM). F. Transwell assays of different HCC cell lines for 24 h. Cells were treated with or without CuET (0.1 μM). G. Qualitative and quantitative analyses of different HCC cell lines treated with or without CuET (0.1 μM) were performed via western blotting to detect changes in the protein levels of EMT-related molecules. n.s: no significant difference, $*p < 0.05$, $**p < 0.01$, $***p < 0.001$ (one-way ANOVA).

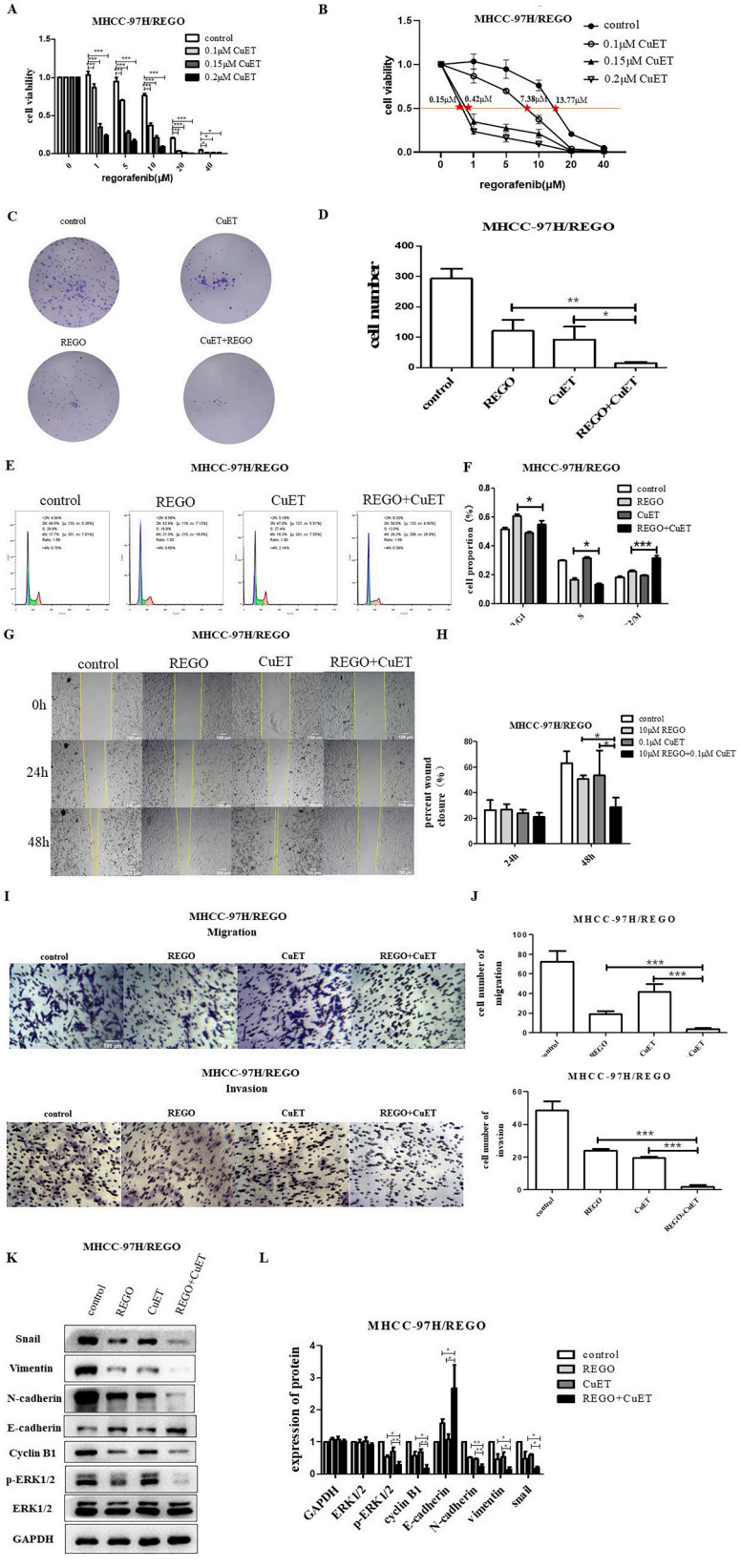

(caption on next page)

Fig. 5. Effect of CuET on the regorafenib sensitivity of regorafenib-resistant HCC cells in vitro.
A. Viability of MHCC-97H/REGO cells cocultured with the indicated concentrations of CuET (0 μM, 0.1 μM, 0.15 μM, 0.2 μM), the indicated concentrations of regorafenib (0 μM, 1 μM, 5 μM, 10 μM, 20 μM, 40 μM) or a combination of the two for 24 h, as determined by the CCK-8 assay. B. The IC50 values of MHCC-97H/REGO cells presented in A are marked (control-13.77 μM, 0.1 μM CuET-7.38 μM, 0.15 μM CuET-0.42 μM, 0.2 μM CuET-0.15 μM). C-D. Colony formation assay on MHCC-97H/REGO cells. Cells were plated at a density of 500 cells per well and then treated with 0.1 μM CuET, 10 μM regorafenib, or a combination of 0.1 μM CuET and 10 μM regorafenib for 24 h. Quantitative analysis was performed. E-F. Cell cycle distributions of control, regorafenib, CuET, or the combination (same drug concentrations as in Figure C) -treated MHCC-97H/REGO cells. Quantitative analysis was subsequently performed. G-H. Wound healing assay of MHCC-97H/REGO cells after treatment with the control, regorafenib, CuET, or the combination (same drug concentrations as in Figure C) for 0 h, 24 h and 48 h. Quantitative analysis of the cell healing rate was performed. I-J. Transwell assay of MHCC-97H/REGO cells at 8×10^4 cells per well. Cells were treated as presented in Figure C before being plated in the Transwell chamber. Quantitative analysis was subsequently performed. K-L. Qualitative and quantitative analyses of the expression levels of proliferation markers and the EMT markers ERK and p-ERK by western blotting. $^*p < 0.05$, $^{**}p < 0.01$, $^{***}p < 0.001$ (one-way ANOVA).

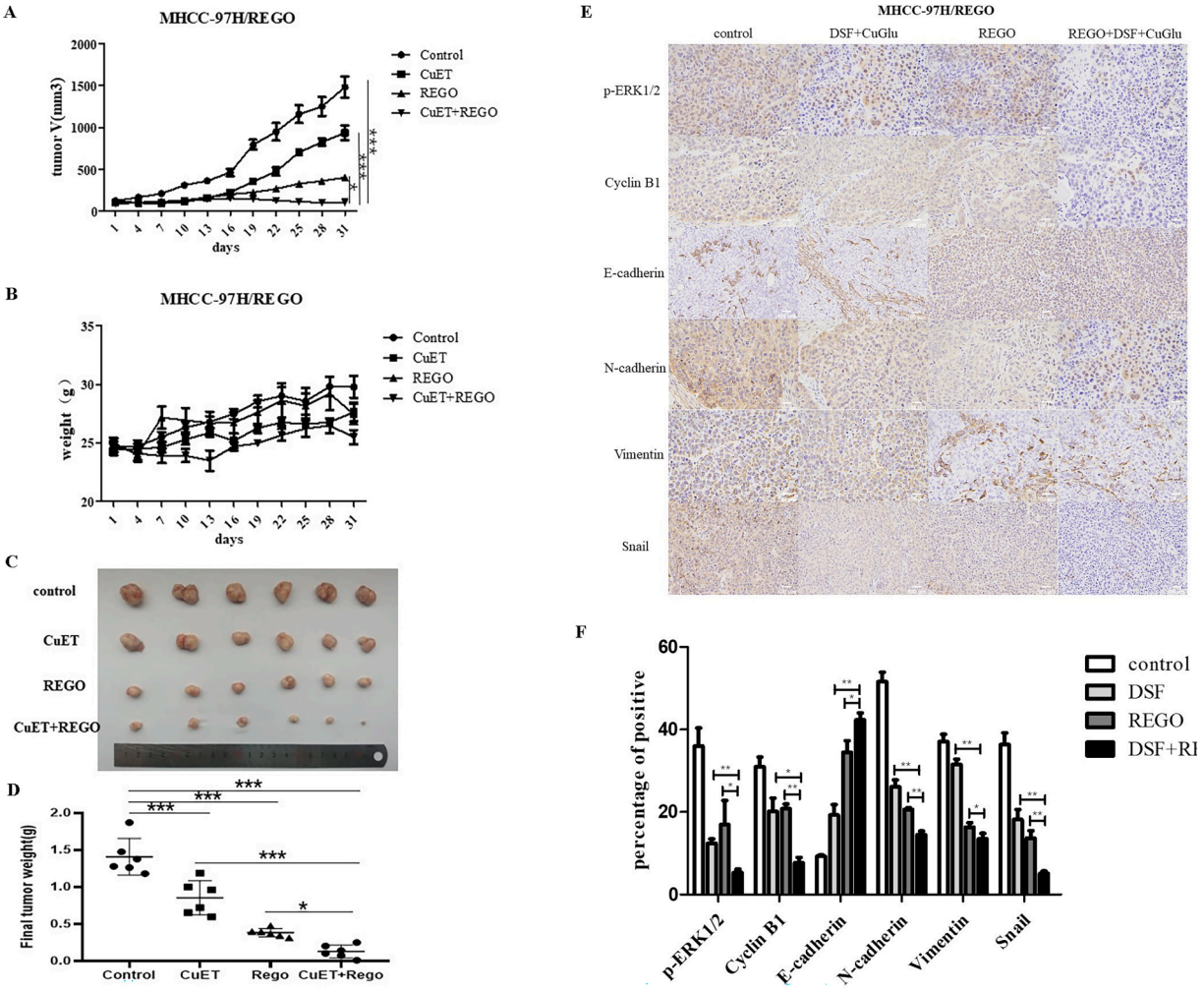

Fig. 6. Effect of CuET on regorafenib sensitivity in MHCC-97H/REGO xenograft models in vivo.
A. Tumor volume was determined every other day. B. Mouse weight was determined every other day. C. Images of tumors harvested from nude mice after sacrifice. D. Final weights of tumors harvested from nude mice. E-F. p-ERK, vimentin, snail, E-cadherin, N-cadherin and cyclin B1 levels were visualized by immunohistochemistry. Quantitative analysis was subsequently performed. $^*p < 0.05$, $^{**}p < 0.01$, $^{***}p < 0.001$ (one-way ANOVA).

Shibue et al. proposed that the process of epithelial-mesenchymal transition (EMT) is considered a critical regulatory factor for the cancer stem cell (CSC) phenotype. They also found that ERK was weakly activated in epithelial cells and highly activated in mesenchymal cells, which is consistent with our results [14]. The EMT phenotype was associated with the acquisition of cisplatin or paclitaxel resistance in A549 cells [36]. Furthermore, drug (doxorubicin) resistance could be reversed by inhibiting EMT [37]. These results suggest that the changes in the EMT phenotype are closely related to the development of drug resistance, and tumor stem cells may play a major role in this process.

We look into the phosphorylation status of all major proteins such as AKT, STAT3 and ERK (Figure S2 and Fig. 2), which are known to trigger EMT. We found that the most obvious change is p-ERK in regorafenib-resistant MHCC-97H/REGO cells (Figure S2 and Fig. 2). FGFR-driven gastric cancer cell lines rapidly reactivate MAPK/ERK signaling in response to FGFR inhibition, which may be the basis of regorafenib's limited clinical response [38]. As an integration point of multiple biochemical signals, ERK participates in a wide variety of cellular processes, such as proliferation, differentiation, migration and development. The activation of ERK requires its phosphorylation [39]. Dysregulation of ERK signaling has recently been shown to be associated with chemoresistance [40]. The expression of p-ERK in sorafenib-resistant HCC cells was significantly higher than that in maternal cells [41]. In our study, a similar phenomenon was found in

regorafenib-resistant cell lines. We observed that the increase in p-ERK in MHCC-97H/REGO cells led to regorafenib resistance, which was also proposed by Zeribe Chike Nwosu et al. Chike Nwosu et al. found that severe metabolic alterations, activation of the ERK pathway, and regorafenib resistance are interrelated, with metabolic dysregulation being the apparent initiating event. In contrast, in this study, prolonged exposure to regorafenib was used as the initiating event, which may suggest that regorafenib has the potential to induce tumor metabolic changes [18]. It was found that lenvatinib resistance could be reversed by inhibiting p-ERK [42]. In our study, we also found that inhibition of p-ERK overcame regorafenib resistance in MHCC-97H/REGO cells. Therefore, ERK pathway intervention could be an important focus in HCC therapy, and further research is needed to understand the changes that occur in the ERK pathway.

CuET is considered to be a promising antitumor drug [24] since research has indicated the feasibility of repurposing the old alcohol-aversion drug DSF for cancer treatment [43]. Some research teams have already started clinical trials to study the antitumor effect of DSF on glioblastoma, non-small cell lung cancer, prostate cancer and so on [44-46]. DSF has been shown to induce the epithelial phenotype and inhibit EMT [26,27]. It has also been shown that DSF inhibits ERK phosphorylation [26]. Therefore, we used DSF to reverse regorafenib resistance in HCC. In this study, we verified the antiproliferative and antimigratory effects of CuET on the regular HCC cell lines SMCC-7721, MHCC-LM3, MHCC-97H, and MHCC-97H/REGO. Xin Huang et al. discovered that CuET inhibits the progression of colorectal cancer. In their study, after the cells were treated with CuET (0.5 μM-1.5 μM), the proliferation of colon cancer cells was inhibited [47]. Liting Ren et al. discovered that CuET inhibits cell migration in breast cancer at the same concentrations (0.1 μM-1 μM) as those used in our study [47]. These findings are consistent with our results.

CuET could also be combined with other drugs to produce more efficient regimens for cancer therapy. The combination of DSF and doxorubicin can effectively inhibit doxorubicin-resistant breast cancer cells [48]. Bing Xu et al. discovered that the DSF/copper complex sensitized doxorubicin-resistant leukemia HL60 cells to cytotoxicity [49], which is consistent with our strategy for treating regorafenib-resistant MHCC-97H/REGO. In this study, we tried a new combination of CuET and regorafenib in MHCC-97H/REGO cells. The combination of these two agents successfully sensitized MHCC-97H/REGO cells.

However, the detailed mechanism through which CuET overcomes the resistance to cancer chemotherapy is still unknown. Regorafenib is a small molecule inhibitor of multiple membrane-bound and intracellular kinases, including, VEGFR1, PDGFR-alpha, FGFR1 and so on [50-52]. In the present study, we found that p-ERK (a downstream effector of VEGFR1, PDGFR-alpha, FGFR1 and other factors [53,54]) was highly expressed regorafenib-resistant HCC cells. Zdenek Skrott et al. reported that CuET inhibits p97-dependent protein degradation [24,52]. Jiaxing Yang et al. found that enhancing DUSP1 expression resulted in a reduction of p-ERK. We hypothesized that CuET can reduce DUSP ubiquitination, thereby leading to a decrease in the p-ERK protein.

In summary, our study revealed that CuET significantly reduced regorafenib resistance in an HCC cell line. This provided us with a valuable strategy to address regorafenib resistance. With the development of clinical trials of DSF, our study may provide new insights into the application of DSF in tumor therapy.

CRediT authorship contribution statement

Ding Ma: Data curation, Formal analysis, Methodology, Software, Writing – original draft. **Shuwen Liu:** Data curation, Investigation, Project administration, Resources. **Kua Liu:** Supervision, Validation, Visualization. **Qinyu He:** Conceptualization, Data curation, Validation. **Lili Hu:** Supervision. **Weiwei Shi:** Supervision. **Yin Cao:** Supervision. **Guang Zhang:** Supervision. **Qilei Xin:** Supervision. **Zhongxia Wang:** Funding acquisition, Supervision, Writing – review & editing. **Junhua Wu:** Conceptualization, Writing – review & editing. **Chunping Jiang:** Conceptualization, Funding acquisition, Writing – review & editing.

Declaration of competing interest

The authors disclose no potential conflicts of interest.

Consent for publication

All authors agree to publish this manuscript.

Funding statement

The research was supported by Shandong Provincial Laboratory Project (SYS202202); the National Natural Science Foundation of China (82272819, 81972888); the Research Project of Jinan Microecological Biomedicine Shandong Laboratory (JNL-202219B, JNL-202204A, JNL-2023017D); the Primary Research & Development Plan of Jiangsu Province (BE2022840); the Open Project of Chinese Materia Medica First-Class Discipline of Nanjing University of Chinese Medicine (2020YLXK007).

Supplementary materials

Supplementary material associated with this article can be found, in the online version, at doi:10.1016/j.tranon.2024.102040.

References

[1] R.L. Siegel, K.D. Miller, H.E. Fuchs, A. Jemal, Cancer Statistics, 2021, CA Cancer J. Clin. 71 (1) (2021) 7–33, https://doi.org/10.3322/caac.21654.
[2] H. Maki, K. Hasegawa, Advances in the surgical treatment of liver cancer, Biosci. Trends 16 (3) (2022) 178–188, https://doi.org/10.5582/bst.2022.01245.
[3] S. Zhu, Y. Wu, X. Zhang, S. Peng, H. Xiao, S. Chen, et al., Targeting N(7)-methylguanosine tRNA modification blocks hepatocellular carcinoma metastasis after insufficient radiofrequency ablation, Mol. Ther. 31 (6) (2023) 1596–1614, https://doi.org/10.1016/j.ymthe.2022.08.004.
[4] D. Anwanwan, S.K. Singh, S. Singh, V. Saikam, R. Singh, Challenges in liver cancer and possible treatment approaches, Biochim. Biophys. Acta Rev. Cancer 1873 (1) (2020) 188314, https://doi.org/10.1016/j.bbcan.2019.188314.
[5] R.S. Finn, P. Merle, A. Granito, Y.H. Huang, G. Bodoky, M. Pracht, et al., Outcomes of sequential treatment with sorafenib followed by regorafenib for HCC: additional analyses from the phase III RESORCE trial, J. Hepatol. 69 (2) (2018) 353–358, https://doi.org/10.1016/j.jhep.2018.04.010.
[6] M.B. Sonbol, I.B. Riaz, S.A.A. Naqvi, D.R. Almquist, S. Mina, J. Almasri, et al., Systemic therapy and sequencing options in advanced hepatocellular carcinoma: a systematic review and network Meta-analysis, JAMA Oncol. 6 (12) (2020) e204930, https://doi.org/10.1001/jamaoncol.2020.4930.
[7] J. Bruix, L.G. da Fonseca, M. Reig, Insights into the success and failure of systemic therapy for hepatocellular carcinoma, Nature Rev. Gastroenterol. Hepatol. 16 (10) (2019) 617–630, https://doi.org/10.1038/s41575-019-0179-x.
[8] S. Napolitano, G. Martini, B. Rinaldi, E. Martinelli, M. Donniacuo, L. Berrino, et al., Primary and acquired resistance of colorectal cancer to Anti-EGFR monoclonal antibody can be overcome by combined treatment of regorafenib with cetuximab, Clin. Cancer Res. 21 (13) (2015) 2975–2983, https://doi.org/10.1158/1078-0432.ccr-15-0020.
[9] A.G. Duffy, T.F. Greten, Liver cancer: regorafenib as second-line therapy in hepatocellular carcinoma, Nature Rev. Gastroenterol. Hepatol. 14 (3) (2017) 141–142, https://doi.org/10.1038/nrgastro.2017.7.
[10] J. Bruix, S. Qin, P. Merle, A. Granito, Y.H. Huang, G. Bodoky, et al., Regorafenib for patients with hepatocellular carcinoma who progressed on sorafenib treatment (RESORCE): a randomised, double-blind, placebo-controlled, phase 3 trial, Lancet 389 (10064) (2017) 56–66, https://doi.org/10.1016/s0140-6736(16)32453-9.
[11] H. Acloque, M.S. Adams, K. Fishwick, M. Bronner-Fraser, M.A. Nieto, Epithelial-mesenchymal transitions: the importance of changing cell state in development and disease, J. Clin. Invest. 119 (6) (2009) 1438–1449, https://doi.org/10.1172/jci38019.
[12] B. Zhou, H. Zhan, L. Tin, S. Liu, J. Xu, Y. Dong, et al., TUFT1 regulates metastasis of pancreatic cancer through HIF1-Snail pathway induced epithelial-mesenchymal transition, Cancer Lett. 382 (1) (2016) 11–20, https://doi.org/10.1016/j.canlet.2016.08.017.
[13] X. Chen, S. Lingala, S. Khoobyari, J. Nolta, M.A. Zern, J. Wu, Epithelial mesenchymal transition and hedgehog signaling activation are associated with chemoresistance and invasion of hepatoma subpopulations, J. Hepatol. 55 (4) (2011) 838–845, https://doi.org/10.1016/j.jhep.2010.12.043.

[14] T. Shibue, R.A. Weinberg, EMT, CSCs, and drug resistance: the mechanistic link and clinical implications, Nature Rev. Clin. Oncol. 14 (10) (2017) 611–629, https://doi.org/10.1038/nrclinonc.2017.44.

[15] M. Singh, N. Yelle, C. Venugopal, S.K. Singh, EMT: mechanisms and therapeutic implications, Pharmacol. Ther. 182 (2018) 80–94, https://doi.org/10.1016/j.pharmthera.2017.08.009.

[16] J. Peng, B.F. Sun, C.Y. Chen, J.Y. Zhou, Y.S. Chen, H. Chen, et al., Single-cell RNA-seq highlights intra-tumoral heterogeneity and malignant progression in pancreatic ductal adenocarcinoma, Cell Res. 29 (9) (2019) 725–738, https://doi.org/10.1038/s41422-019-0195-y.

[17] M. Olea-Flores, M.D. Zuñiga-Eulogio, M.A. Mendoza-Catalán, H.A. Rodríguez-Ruiz, E. Castañeda-Saucedo, C. Ortuño-Pineda, et al., Extracellular-signal regulated kinase: a central molecule driving epithelial-mesenchymal transition in cancer, Int. J. Mol. Sci. 20 (12) (2019), https://doi.org/10.3390/ijms20122885.

[18] Z.C. Nwosu, W. Piorońska, N. Battello, A.D. Zimmer, B. Dewidar, M. Han, et al., Severe metabolic alterations in liver cancer lead to ERK pathway activation and drug resistance, EBioMedicine 54 (2020) 102699, https://doi.org/10.1016/j.ebiom.2020.102699.

[19] J. Ma, S. Zeng, Y. Zhang, G. Deng, Y. Qu, C. Guo, et al., BMP4 promotes oxaliplatin resistance by an induction of epithelial-mesenchymal transition via MEK1/ERK/ELK1 signaling in hepatocellular carcinoma, Cancer Lett. 411 (2017) 117–129, https://doi.org/10.1016/j.canlet.2017.09.041.

[20] S.M. Akula, S.L. Abrams, L.S. Steelman, M.R. Emma, G. Augello, A. Cusimano, et al., RAS/RAF/MEK/ERK, PI3K/PTEN/AKT/mTORC1 and TP53 pathways and regulatory miRs as therapeutic targets in hepatocellular carcinoma, Expert Opin. Ther. Targets 23 (11) (2019) 915–929, https://doi.org/10.1080/14728222.2019.1685501.

[21] A.M. Czarnecka, E. Bartnik, M. Fiedorowicz, P. Rutkowski, Targeted Therapy in Melanoma and Mechanisms of Resistance, Int. J. Mol. Sci. 21 (13) (2020), https://doi.org/10.3390/ijms21134576.

[22] K. Iljin, K. Ketola, P. Vainio, P. Halonen, P. Kohonen, V. Fey, et al., High-throughput cell-based screening of 4910 known drugs and drug-like small molecules identifies disulfiram as an inhibitor of prostate cancer cell growth, Clin. Cancer Res. 15 (19) (2009) 6070–6078, https://doi.org/10.1158/1078-0432.Ccr-09-1035.

[23] W. Wu, L. Yu, Q. Jiang, M. Huo, H. Lin, L. Wang, et al., Enhanced tumor-specific disulfiram chemotherapy by In Situ Cu(2+) chelation-initiated nontoxicity-to-toxicity transition, J. Am. Chem. Soc. 141 (29) (2019) 11531–11539, https://doi.org/10.1021/jacs.9b03503.

[24] Z. Skrott, M. Mistrik, K.K. Andersen, S. Friis, D. Majera, J. Gursky, et al., Alcohol-abuse drug disulfiram targets cancer via p97 segregase adaptor NPL4, Nature 552 (7684) (2017) 194–199, https://doi.org/10.1038/nature25016.

[25] M. Viola-Rhenals, K.R. Patel, L. Jaimes-Santamaria, G. Wu, J. Liu, Q.P. Dou, Recent advances in antabuse (Disulfiram): the importance of its metal-binding ability to its anticancer activity, Curr. Med. Chem. 25 (4) (2018) 506–524, https://doi.org/10.2174/0929867324666171023161121.

[26] D. Han, G. Wu, C. Chang, F. Zhu, Y. Xiao, Q. Li, et al., Disulfiram inhibits TGF-β-induced epithelial-mesenchymal transition and stem-like features in breast cancer via ERK/NF-κB/Snail pathway, Oncotarget. 6 (38) (2015) 40907–40919, https://doi.org/10.18632/oncotarget.5723.

[27] Y. Li, L.H. Wang, H.T. Zhang, Y.T. Wang, S. Liu, W.L. Zhou, et al., Disulfiram combined with copper inhibits metastasis and epithelial-mesenchymal transition in hepatocellular carcinoma through the NF-κB and TGF-β pathways, J. Cell. Mol. Med. 22 (1) (2018) 439–451, https://doi.org/10.1111/jcmm.13334.

[28] Y. Pang, S.S. Mao, R. Yao, J.Y. He, Z.Z. Zhou, L. Feng, et al., TGF-β induced epithelial-mesenchymal transition in an advanced cervical tumor model by 3D printing, Biofabrication. 10 (4) (2018) 044102, https://doi.org/10.1088/1758-5090/aadbde.

[29] R. Bista, D.W. Lee, O.B. Pepper, D.O. Azorsa, R.J. Arceci, E. Aleem, Disulfiram overcomes bortezomib and cytarabine resistance in Down-syndrome-associated acute myeloid leukemia cells, J. Exp. Clin. Cancer Res.: CR 36 (1) (2017) 22, https://doi.org/10.1186/s13046-017-0493-5.

[30] L. Ren, W. Feng, J. Shao, J. Ma, M. Xu, B.Z. Zhu, et al., Diethyldithiocarbamate-copper nanocomplex reinforces disulfiram chemotherapeutic efficacy through light-triggered nuclear targeting, Theranostics. 10 (14) (2020) 6384–6398, https://doi.org/10.7150/thno.45558.

[31] Z. Chen, W. Yu, Q. Zhou, J. Zhang, H. Jiang, D. Hao, et al., A novel lncRNA IHS promotes tumor proliferation and metastasis in HCC by regulating the ERK- and AKT/GSK-3β-signaling pathways, Mol. Therapy Nucleic Acids 16 (2019) 707–720, https://doi.org/10.1016/j.omtn.2019.04.021.

[32] Y.A. Heo, Y.Y. Syed, Regorafenib: a review in hepatocellular carcinoma, Drugs 78 (9) (2018) 951–958, https://doi.org/10.1007/s40265-018-0932-4.

[33] M. Tong, N. Che, L. Zhou, S.T. Luk, P.W. Kau, S. Chai, et al., Efficacy of annexin A3 blockade in sensitizing hepatocellular carcinoma to sorafenib and regorafenib, J. Hepatol. 69 (4) (2018) 826–839, https://doi.org/10.1016/j.jhep.2018.05.034.

[34] X. Song, L. Shen, J. Tong, C. Kuang, S. Zeng, R.E. Schoen, et al., Mcl-1 inhibition overcomes intrinsic and acquired regorafenib resistance in colorectal cancer, Theranostics. 10 (18) (2020) 8098–8110, https://doi.org/10.7150/thno.45363.

[35] M. Karabicici, Y. Azbazdar, G. Ozhan, S. Senturk, Z. Firtina Karagonlar, E Erdal, Changes in Wnt and TGF-β signaling mediate the development of regorafenib resistance in hepatocellular carcinoma cell line HuH7, Front. Cell Dev. Biol. 9 (2021) 639779, https://doi.org/10.3389/fcell.2021.639779.

[36] M.L. Han, Y.F. Zhao, C.H. Tan, Y.J. Xiong, W.J. Wang, F. Wu, et al., Cathepsin L upregulation-induced EMT phenotype is associated with the acquisition of cisplatin or paclitaxel resistance in A549 cells, Acta Pharmacol. Sin. 37 (12) (2016) 1606–1622, https://doi.org/10.1038/aps.2016.93.

[37] J. Xu, D. Liu, H. Niu, G. Zhu, Y. Xu, D. Ye, et al., Resveratrol reverses Doxorubicin resistance by inhibiting epithelial-mesenchymal transition (EMT) through modulating PTEN/Akt signaling pathway in gastric cancer, J. Exp. Clin. Cancer Res.: CR 36 (1) (2017) 19, https://doi.org/10.1186/s13046-016-0487-8.

[38] D.K. Lau, I.Y. Luk, L.J. Jenkins, A. Martin, D.S. Williams, K.L. Schoffer, et al., Rapid resistance of FGFR-driven gastric cancers to regorafenib and targeted FGFR inhibitors can be overcome by parallel inhibition of MEK, Mol. Cancer Ther. 20 (4) (2021) 704–715, https://doi.org/10.1158/1535-7163.mct-20-0836.

[39] K.D. Pruitt, G.R. Brown, S.M. Hiatt, F. Thibaud-Nissen, A. Astashyn, O. Ermolaeva, et al., RefSeq: an update on mammalian reference sequences, Nucleic Acids Res. 42 (Database issue) (2014) D756–D763, https://doi.org/10.1093/nar/gkt1114.

[40] Z. Chen, Q. Chen, Z. Cheng, J. Gu, W. Feng, T. Lei, et al., Long non-coding RNA CASC9 promotes gefitinib resistance in NSCLC by epigenetic repression of DUSP1, Cell Death Dis 11 (10) (2020) 858, https://doi.org/10.1038/s41419-020-03047-y.

[41] C.O.N. Leung, M. Tong, K.P.S. Chung, L. Zhou, N. Che, K.H. Tang, et al., Overriding adaptive resistance to sorafenib through combination therapy with Src homology 2 domain-containing phosphatase 2 blockade in hepatocellular carcinoma, Hepatology (Baltimore, Md) 72 (1) (2020) 155–168, https://doi.org/10.1002/hep.30989.

[42] Z. Zhao, D. Zhang, F. Wu, J. Tu, J. Song, M. Xu, et al., Sophoridine suppresses lenvatinib-resistant hepatocellular carcinoma growth by inhibiting RAS/MEK/ERK axis via decreasing VEGFR2 expression, J. Cell. Mol. Med. 25 (1) (2021) 549–560, https://doi.org/10.1111/jcmm.16108.

[43] D. Majera, Z. Skrott, K. Chroma, J.M. Merchut-Maya, M. Mistrik, J. Bartek, Targeting the NPL4 adaptor of p97/VCP Segregase by disulfiram as an emerging cancer vulnerability evokes replication stress and DNA Damage while Silencing the ATR pathway, Cells 9 (2) (2020), https://doi.org/10.3390/cells9020469.

[44] J. Huang, R. Chaudhary, A.L. Cohen, K. Fink, S. Goldlust, J. Boockvar, et al., A multicenter phase II study of temozolomide plus disulfiram and copper for recurrent temozolomide-resistant glioblastoma, J. Neurooncol. 142 (3) (2019) 537–544, https://doi.org/10.1007/s11060-019-03125-y.

[45] H. Nechushtan, Y. Hamamreh, S. Nidal, M. Gotfried, A. Baron, Y.I. Shalev, et al., A phase IIb trial assessing the addition of disulfiram to chemotherapy for the treatment of metastatic non-small cell lung cancer, Oncologist 20 (4) (2015) 366–367, https://doi.org/10.1634/theoncologist.2014-0424.

[46] M.T. Schweizer, J. Lin, A. Blackford, A. Bardia, S. King, A.J. Armstrong, et al., Pharmacodynamic study of disulfiram in men with non-metastatic recurrent prostate cancer, Prostate Cancer Prostatic Dis. 16 (4) (2013) 357–361, https://doi.org/10.1038/pcan.2013.28.

[47] X. Huang, Y. Hou, X. Weng, W. Pang, L. Hou, Y. Liang, et al., Diethyldithiocarbamate-copper complex (CuET) inhibits colorectal cancer progression via miR-16-5p and 15b-5p/ALDH1A3/PKM2 axis-mediated aerobic glycolysis pathway, Oncogenesis. 10 (1) (2021) 4, https://doi.org/10.1038/s41389-020-00295-7.

[48] F. Rolle, V. Bincoletto, E. Gazzano, B. Rolando, G. Lollo, B. Stella, et al., Coencapsulation of disulfiram and doxorubicin in liposomes strongly reverses multidrug resistance in breast cancer cells, Int. J. Pharm. 580 (2020) 119191, https://doi.org/10.1016/j.ijpharm.2020.119191.

[49] B. Xu, P. Shi, I.S. Fombon, Y. Zhang, F. Huang, W. Wang, et al., Disulfiram/copper complex activated JNK/c-jun pathway and sensitized cytotoxicity of doxorubicin in doxorubicin resistant leukemia HL60 cells, Blood Cells Mol. Dis. 47 (4) (2011) 264–269, https://doi.org/10.1016/j.bcmd.2011.08.004.

[50] A. Jindal, A. Thadi, K. Shailubhai, Hepatocellular carcinoma: etiology and current and future drugs, J. Clin. Exp. Hepatol. 9 (2) (2019) 221–232, https://doi.org/10.1016/j.jceh.2019.01.004.

[51] C. Serrano, S. Bauer, D. Gómez-Peregrina, Y.K. Kang, R.L. Jones, P. Rutkowski, et al., Circulating tumor DNA analysis of the phase III VOYAGER trial: KIT mutational landscape and outcomes in patients with advanced gastrointestinal stromal tumor treated with avapritinib or regorafenib, Ann. Oncol. 34 (7) (2023) 615–625, https://doi.org/10.1016/j.annonc.2023.04.006.

[52] Ettrich T.J., Seufferlein T. Regorafenib. *Recent results in cancer research Fortschritte der Krebsforschung Progres dans les recherches sur le cancer* 2014;201:185–96 doi 10.1007/978-3-642-54490-3_10.

[53] A. Sadremomtaz, F. Kobarfard, K. Mansouri, L. Mirzanejad, S.M. Asghari, Suppression of migratory and metastatic pathways via blocking VEGFR1 and VEGFR2, J. Recept. Signal Transduct. Res. 38 (5–6) (2018) 432–441, https://doi.org/10.1080/10799893.2019.1567785.

[54] F. Perrone, L. Da Riva, M. Orsenigo, M. Losa, G. Jocollè, C. Millefanti, et al., PDGFRA, PDGFRB, EGFR, and downstream signaling activation in malignant peripheral nerve sheath tumor, Neuro-Oncology 11 (6) (2009) 725–736, https://doi.org/10.1215/15228517-2009-003.